energies

MDPI

Article

Laminar Burning Velocities of Hydrogen-Blended Methane–Air and Natural Gas–Air Mixtures, Calculated from the Early Stage of $p(t)$ Records in a Spherical Vessel

Maria Mitu [1,*], Domnina Razus [1] and Volkmar Schroeder [2]

[1] "Ilie Murgulescu" Institute of Physical Chemistry, Romanian Academy, 202 Spl. Independentei, 060021 Bucharest, Romania; drazus@icf.ro
[2] Formerly Bundesanstalt fuer Materialforschung und-Pruefung (BAM), Unter den Eichen 87, 12205 Berlin, Germany; vk.schroeder@gmx.de
* Correspondence: maria_mitu@icf.ro

Abstract: The flammable hydrogen-blended methane–air and natural gas–air mixtures raise specific safety and environmental issues in the industry and transportation; therefore, their explosion characteristics such as the explosion limits, explosion pressures, and rates of pressure rise have significant importance from a safety point of view. At the same time, the laminar burning velocities are the most useful parameters for practical applications and in basic studies for the validation of reaction mechanisms and modeling turbulent combustion. In the present study, an experimental and numerical study of the effect of hydrogen addition on the laminar burning velocity (LBV) of methane–air and natural gas–air mixtures was conducted, using mixtures with equivalence ratios within 0.90 and 1.30 and various hydrogen fractions r_H within 0.0 and 0.5. The experiments were performed in a 14 L spherical vessel with central ignition at ambient initial conditions. The LBVs were calculated from $p(t)$ data, determined in accordance with EN 15967, by using only the early stage of flame propagation. The results show that hydrogen addition determines an increase in LBV for all examined binary flammable mixtures. The LBV variation versus the fraction of added hydrogen, r_H, follows a linear trend only at moderate hydrogen fractions. The further increase in r_H results in a stronger variation in LBV, as shown by both experimental and computed LBVs. Hydrogen addition significantly changes the thermal diffusivity of flammable CH_4–air or NG–air mixtures, the rate of heat release, and the concentration of active radical species in the flame front and contribute, thus, to LBV variation.

Keywords: hydrogen; methane; natural gas; laminar burning velocity (LBV); closed vessel combustion

Citation: Mitu, M.; Razus, D.; Schroeder, V. Laminar Burning Velocities of Hydrogen-Blended Methane–Air and Natural Gas–Air Mixtures, Calculated from the Early Stage of $p(t)$ Records in a Spherical Vessel. *Energies* **2021**, *14*, 7556. https://doi.org/10.3390/en14227556

Academic Editors: Adonios Karpetis and Giancarlo Sorrentino

Received: 16 September 2021
Accepted: 8 November 2021
Published: 12 November 2021

1. Introduction

In recent years, dependence on fossil fuels as the main energy source has led to a worldwide crisis, due to fossil fuel depletion, and environmental problems due to pollutant emissions have become severe. To respond to these problems, continuous attempts have been made in the exploration of clean, renewable alternatives for sustainable development [1,2]. The research on alternative fuels is mainly focused on natural gas [3–7], hydrogen [8–15], and alcohols [16,17], able to be mixed with gasoline, diesel, or to form mutual blends.

The extended use of natural gas (NG) as fuel in internal combustion (IC) and gas turbines prompted numerous research groups to examine its combustion in air, under various initial conditions (NG/air ratio, pressure, temperature, additives) [4–6]. A common practice in NG use is its blending with hydrogen. Hydrogen has attracted the attention of researchers as a renewable clean energy source. Hydrogen is easily ignitable and its flame spreads quickly, which is essential for IC engines to order to work under an improved combustion efficiency [7–15]. Hydrogen addition to NG is a good option for

decreasing CO, CO_2, and NO_x emissions, especially for fuel-lean mixtures [18]. Other effects of H_2 addition to NG are the stabilizing effect on lean NG–air flames, along with an increased risk of flame flash-back in burners originally designed for natural gas [3,19]. Hydrogen raises numerous safety issues, especially when mixed with other flammable gases. The main cause of such effects is the higher reactivity of H_2 compared to each C_1–C_4 alkanes from NG, resulting in important variations of ignition and propagation characteristic parameters of NG–air combustion: decreases in ignition delay times of self-ignition and minimum ignition energies, increases in adiabatic flame temperature and in laminar burning velocity [9,11,20,21]. Taking into account the variable composition of NG as a result of current changes in its supplies, many studies were conducted on CH_4/H_2/air flames [8,11,13,14,19–32]. Such studies revealed the effect of H_2 enrichment: enlargement of the flammability range of CH_4–air mixtures [11,13,14], decreases in ignition delay times in jet-stirred reactors, rapid compression machines or shock tubes [21,26,30], decreases in maximum experimental safe gap (MESG) [11], and increases in flame speed and laminar burning velocity [8,22–32]. Another beneficial effect of enriching methane with hydrogen consists of the increase in flame resistance to strain-induced extinction, as highlighted by Di Sarli et al. [33,34]. Di Sarli et al. investigated a hythane lean and stoichiometric mixture with hydrogen mole fraction in the fuel, r_{H2}, within 0–0.5 using time-resolved particle image velocimetry (PIV). The authors discussed the interactions that occur between the flame front and the observed toroidal vortex structures [33]. For the same hydrogen-enriched methane/air premixed flames, Di Sarli and Di Benedetto investigated the effects of non-equidiffusion on their unsteady propagation [34]. Numerical studies of flame ignition and propagation also outlined the increase in reactivity determined by H_2 addition and discussed the pathways of CH_4–H_2 oxidation in air, as compared to CH_4 oxidation [3,7,18,19,26,30,32,35].

Experimental and numerical studies were conducted on NG/H_2/air flames as well at various ratios [NG] to [H_2], overall equivalence ratios, and initial pressures and temperatures, using stationary flames or outwardly propagating non-stationary flames, in both unconfined and confined conditions [7,9,11,13,18,26,30–42].

Studies of closed vessel explosions delivered the characteristic parameters of flame propagation under confined conditions (the maximum explosion pressure p_{max}, the explosion delay time θ_{max}, the maximum rate of pressure rise $(dp/dt)_{max}$, and deflagration index K_G) for NG and H_2-blended NG [11,13,29,43]. Closed vessel experiments offer the necessary information for laminar burning velocity determination. This is a highly examined topic, since laminar burning velocities are key factors for validation of detailed mechanisms of fuel–air combustion. Studies of outwardly spherical flames based on transient records of flame radius and pressure [8,22,25–30,36–42] were reported for H_2-blended CH_4 and H_2-blended NG with variable initial composition (variable [H_2]/[CH_4] and [H_2]/[NG] ratios or variable equivalence ratios), initial pressure, or initial temperature. Additional information on flame structure (temperature and chemical species profiles) able to enlighten the influence of H_2 addition on hydrocarbon fuel combustion is found in studies on stationary flames [19,23,24,28,31,32,41].

The conventional combustion of either pure methane or of its blends with hydrogen raises several issues related to emissions of high pollutants such as NO_x. Such issues, associated with the dense energy input caused by preheating the flammable mixtures, can be solved by some new technologies, as suggested in recent articles describing MILD (flameless) combustion [44,45]. The flameless combustion of CH_4/H_2 in a laboratory-scaled furnace was investigated by Cellek [44], proving this is an effective way to reduce pollutant emissions despite the intense energy induced by air preheating, which causes higher flame temperatures. Even when various inlet operating conditions are used, outside canonical configurations (e.g., inside a small-scale device), the specific MILD advantage can be obtained by an adequate degree of dilution, as outlined by Cerello et al. [45].

The aim of the present work is to examine hydrogen influence on laminar burning velocity for different methane/hydrogen and natural gas/hydrogen mixtures with air at

ambient initial conditions. For this, $p(t)$ data obtained in experimental investigations were used. These measurements, performed according to European Standards EN 15967 [46], were originally conducted to determine the maximum explosion pressure p_{max}, the maximum rate of pressure rise $(dp/dt)_{max}$, and the deflagration index K_G. The paper reports LBVs of hydrogen-blended methane–air and natural gas–air mixtures, using mixtures at ambient initial pressure and temperature (p_0 = 0.97–1.04 bar, T_0 = 22–25 °C). The mixtures being studied consist of single fuel–air (CH_4–air) and multifuel–air mixtures, where the multifuel was CH_4 blended with H_2, or natural gas blended with H_2, both under various amounts of added hydrogen, within 0–50 mol% (in respect to the initial fuel amount). The studied systems had either a constant fuel (CH_4 or NG)/H_2 ratio and a variable equivalence ratio or a variable fuel (CH_4 or NG)/H_2 ratio and a constant equivalence ratio. Their laminar burning velocities were determined from the cubic law constants, evaluated from $p(t)$ records obtained in the early stage of closed vessel explosions. Thus, the LBV of H_2-blended CH_4–air and NG–air were determined from single $p(t)$ records, without the additional optical methods of investigation, and were found to describe well the behavior of these multifuel mixtures.

The present results represent a contribution to the data pool regarding the flame propagation in hydrogen-blended CH_4/air and NG/air mixtures. Earlier studies [47,48] provided data for risk assessment at gas processing facilities, especially those involving the introduction of hydrogen into existing natural gas networks under project NATURALHY financed by the EU. The unwanted consequences of such events, i.e., loss of assets, human injuries, fatalities, or severe environmental impacts, can be avoided by a proper safety analysis based on experiments, as discussed by Amin et al. [49].

2. Experimental Procedure

The experiments were conducted at BAM as part of a systematic investigation on safety-related characteristics of natural gas–hydrogen mixtures [11,43]. The pressure–time curves obtained during the determination of explosion limits, explosion pressures, and deflagration constants (K_G) could be used directly to calculate the LBVs using the method described below. The laboratory set-up was previously described in detail [11]. The set-up affords the monitoring of closed vessel explosions for gaseous mixtures of variable composition, pressure, and temperature. A 14 L spherical vessel with central ignition was used to perform experiments with quiescent gas mixtures. An exploding wire igniter (nickeline wire, diameter: 0.12 mm, distance of electrodes: 5 mm) delivered about 15 J for ignition. The ignition systems used are in accordance with EN 1839 [50].

The pressure measurements were made with piezoresistive pressure transducers, type PAA10 (Keller). For mixture preparation pressure transducers with a measuring range between 0 bar (abs) and 2 bar (abs) or between 0 bar (abs) and 5 bar (abs) were used. For measuring the explosion pressure, pressure transducers with a measuring range between 0 bar (abs) and 10 bar (abs) were used. The measuring frequency was 20,000 Hz. The digitized signals of the measuring sensors were connected to an A/D converter, type MCL-USB (16 channels, 16 Bit A/D, sampling frequency: 500 kHz, from Jet Systemtechnik GmbH) and a PC for displaying, storing, and evaluating the data.

Two types of European natural gas were tested: one representing a typical Russian natural gas composition, nearly pure methane, and one of wet type containing CH_4 and a significant amount of C_2–C_4 alkanes, similar to Northern Sea natural gas [11]. The composition of the studied natural gas is given in Table 1.

Table 1. Composition of studied wet natural gas.

Component	CH_4	C_2H_6	C_3H_8	n-C_4H_{10}
Fraction in NG, mol%	89.3	8.0	2.0	0.7

Using pure CH_4 and wet natural gas blended with H_2, multifuel–air mixtures of variable hydrogen content and equivalence ratio were studied at ambient initial pressure and temperature. Their composition is given in Table 2. The hydrogen content in the initial flammable mixture is expressed as the fraction r_H, defined as:

$$r_H = \frac{[H_2]}{([CH_4] + [H_2])} \text{ or } r_H = \frac{[H_2]}{([NG] + [H_2])} \quad (1)$$

The equivalence ratio, φ, of any flammable mixture is defined as:

$$\varphi = \frac{\frac{[\text{fuel}]}{[\text{oxygen}]}}{\left(\frac{[\text{fuel}]}{[\text{oxygen}]}\right)_{\text{st}}}$$

where the index "st" refers to the stoichiometric concentration of the fuel–air mixture.

Table 2. Studied systems (fraction of H_2, r_H, and equivalence ratios, φ).

Fuel	r_H	Equivalence Ratios, φ
CH_4–air	0	0.95–1.15
CH_4–H_2–air	0.05; 0.10; 0.25; 0.50	0.90–1.30
Natural gas (NG)–air	0	0.90–1.20
Natural gas (NG)–H_2–air	0.10; 0.25; 0.50	0.95–1.15

The mixtures of CH_4 or NG with different fractions of hydrogen and air were prepared in a pressure resistant stainless-steel vessel, according to the partial pressure method at total pressure of 2 bar or 5 bar, assuming an ideal gas behavior for all gaseous components.

3. Computing Program

The burning velocities of fuel–air and multifuel–air systems, at ambient initial conditions, were delivered by the kinetic modeling of their flames using COSILAB software (version 3.0.3) and Gas Research Institute (GRI) mechanism version 3.0 [51], where 53 chemical species and 325 elementary reactions are taken into account. The input data were taken from the thermodynamic and molecular databases of Sandia National Laboratories, USA, according to the international standard (format for CHEMKIN). The runs were performed for premixed 1D adiabatic laminar free flames of stoichiometric CH_4–air, NG–air, and H_2-blended mixtures at ambient initial conditions. In these runs, a steady Newton solver (25 iterations, relative tolerance 10^{-5}; absolute tolerance 10^{-8}), an unsteady Newton solver (15 iterations, relative tolerance 10^{-4}; absolute tolerance 10^{-6}), and an unsteady Euler solver were used, as mentioned earlier [52,53]. The parameters of the adaptive grid were GRAD = 0.1, CURV = 0.2, with a maximum ratio of adjacent cell size between 1.3 and 1.1.

4. Data Evaluation

The pressure rise in the early stage of closed vessel explosions, Δp, was found to increase with time from ignition, t, according to so-called "cubic law" [52,54]:

$$\text{or } r_H = \frac{[H_2]}{([NG] + [H_2])} \quad (2)$$

The equation is valid as long as the spherical propagation of the combustion wave is not disturbed. In small-scale explosions, the flame front of reactive mixtures does not develop significant cellular structures and no gas turbulence appears. Indeed, the pressure rise Δp was found proportional to t^3 in quiescent conditions of combustion (CH_4–air, at p_0 = 1 bar (Dobashi [55]) and aviation grade JP-4 fuel with air, at p_0 = 135–275 bar (Knapton

et al. [56]) and to $t^{3.6-6.0}$ in turbulent conditions (CH_4–air, at p_0 = 1 bar (Dobashi [55]). In large-scale explosions (vessels with a volume between 1 and 10 m_3), where the buoyancy effect determines the distortion of the flame, even in the early stage, the time exponent varied between 3.3 and 5.0 for stoichiometric CH_4–air mixtures diluted with various amounts of nitrogen (Sapko et al. [57]).

Assuming the isothermal compression of unburned gas ahead the flame front, the laminar burning velocity, S_u, was related to k, the cubic law coefficient of pressure rise by the relationship [54]:

$$S_u = R \cdot \left(\frac{k}{\Delta p_{max}}\right)^{\frac{1}{3}} \left(\frac{p_0}{p_{max}}\right)^{\frac{2}{3}} \quad (3)$$

where R is the radius of the explosion vessel, Δp_{max} is the peak pressure rise in the explosion at the initial pressure p_0, and $p_{max} = \Delta p_{max} + p_0$. The measured values of Δp_{max} and p_{max} are used as input values for S_u calculation.

The cubic law coefficient can be determined for each experiment over a restricted pressure range ($p_0 \leq p \leq 2p_0$) using a nonlinear regression method with a relationship of the form:

$$\Delta p = a + k\,(t - c)^3 \quad (4)$$

where a and c are corrections for pressure and time, respectively, necessary for eliminating the signal shift of the pressure transducer and the possible delay in signal triggering [52]. Smaller residuals and a random error distribution, indicating better correlations, were obtained by using this modified Equation (4), instead of Equation (2).

The method was successfully used for determining LVBs of various hydrocarbon-oxidizer mixtures [52–54,58–61] under various initial conditions of pressure and/or temperature.

5. Results and Discussion

A set of experimental burning velocities of CH_4–H_2–air mixtures obtained from $p(t)$ measurements in a closed spherical vessel at ambient initial pressure, temperature, and constant r_H, is given in Table 3.

Table 3. Typical values of Su for H_2-blended CH_4 mixed with air at r_H = 0.25.

[CH_4]/mol%	[H_2]/mol%	[CH_4 + H_2]/mol%	Equivalence Ratio, φ	S_u/(cm s^{-1})
8.40	2.80	11.20	0.978	58.6
8.84	2.96	11.80	1.037	61.0
9.14	3.06	12.20	1.077	60.2
9.14	3.06	12.20	1.077	60.9
9.14	3.06	12.20	1.077	61.9
9.30	3.10	12.40	1.098	61.6
9.44	3.16	12.60	1.117	58.6
9.60	3.20	12.80	1.139	58.0
10.04	3.33	13.40	1.199	51.5
10.50	3.50	14.00	1.263	45.6

The influence of the initial composition (characterized by r_H and φ) on experimental laminar burning velocities is shown in Figure 1, where data referring to CH_4–H_2–air and NG–H_2–air mixtures are given. The burning velocities of all mixtures increase by increasing the equivalence ratio and reaching their peak values, then start to decrease at higher equivalence ratios. The LBV variation due to H_2 addition is observed already at r_H = 0.05 for lean CH_4–air mixtures. In the range of rich CH_4–air and NG–air mixtures, the LBV changes significantly only at r_H > 0.10. For higher hydrogen contents (r_H = 0.25 and 0.50), a marked increase in LBV appears over the whole examined range of equivalence ratios.

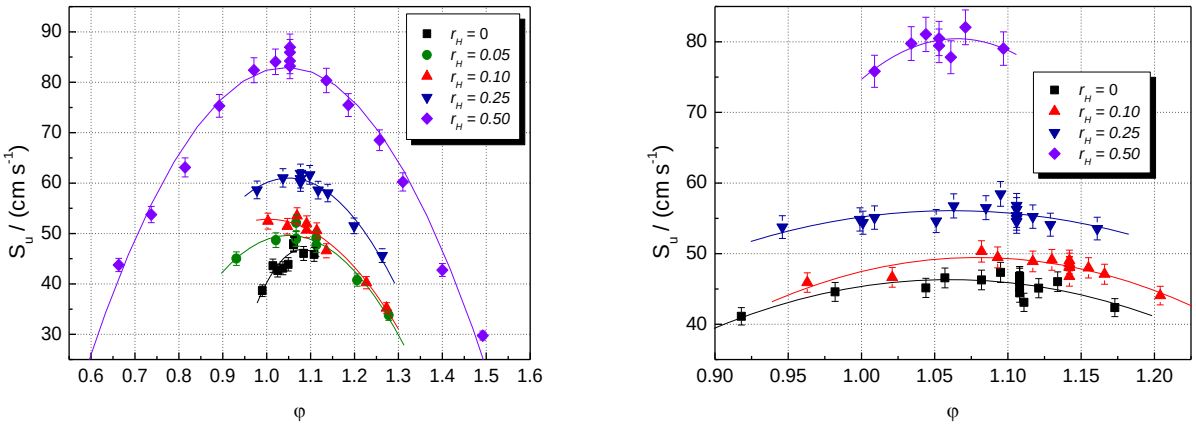

Figure 1. Experimental laminar burning velocities of single fuel–air and multifuel–air mixtures with various r_H at ambient initial pressure and temperature: (**a**) CH_4–H_2–air; (**b**) NG–H_2–air mixtures (present data).

The LBV of the stoichiometric CH_4–air mixture is S_u = 40 cm s^{-1}, in good agreement with most literature data: S_u = 41.2 cm s^{-1} [62], 41.0 cm s^{-1} [6], 40 cm s^{-1} [5], and 38 cm s^{-1} [53]. For this stoichiometric CH_4–air mixture, the earlier reported LBVs vary within 35 and 41.5 cm s^{-1} [4–6,62] at ambient initial conditions, a domain where the present values range well. For the stoichiometric NG–air mixture, the LBV is S_u = 45.7 cm s^{-1}, close to 44.0 cm s^{-1}, previously reported [6,37].

Hydrogen addition to CH_4 or NG results in an increase in S_u at all initial concentrations of CH_4 or NG. The blended mixtures (CH_4–H_2 or NG–H_2) with a constant [H_2] having various equivalence ratios develop the maxima of their burning velocities at slightly rich mixtures, with $\varphi = 1.05 \pm 0.05$.

Both datasets were well fitted by 2nd order polynomials, plotted as well in Figure 1. The points are scattered around the best-fit lines; a possible cause is the turbulence created already in the early stage of explosion by the ignition, made by a strong initiation source (exploding wires, which delivered 15 J). This turbulence could determine deviations from the spherical propagation and errors of the model used. Other methods were also used to extract the laminar burning velocity from transient pressure measurements [63–67]. These methods require equilibrium calculations of unburned and burned gas states to determine LBV using the transient burned mass fraction. They are rigorous methods, which also deliver the temperature gradients in the burned gas and afford the evaluation of the flame stretch effect on burning velocity. In comparison with them, the actual method for determining LBVs from pressure measurements in the early stage of explosion propagation has the advantage of delivering LBVs without additional computations and without additional experimental techniques for measuring the flame radius. This aspect is an advantage when flammable mixtures of multifuels or multi-oxidizers are examined, and the thermodynamic calculations of the intermediate states are impossible or very difficult.

Examination of literature on LBV of H_2-blended CH_4–air and NG–air mixtures provides a wide database of comparison. All datasets show the same variation of burning velocities when examined as a function of the equivalence ratio (at constant r_H) or function of r_H (at constant φ) [3,7,19,21,23,27–30,37,38,68,69]. Differences arise among measurements performed using different techniques, involving various corrections of the recorded information.

A closer examination of present results compared with literature data can be made by examining the LBV of stoichiometric CH_4–air and NG–air mixtures blended with hydrogen at various fractions of added H_2, as shown by the plots given in Figure 2. With respect to CH_4–H_2–air mixtures (Figure 2a), the present results are found to match well with those obtained as stretch-free LBV, using the technique of counter-flow flames [23]. For the

examined range of the fraction of added hydrogen, $r_H \leq 0.5$, they seem to depend linearly on it. The same holds for the other datasets, obtained mostly with stationary flames using the heat flux technique [4,24,28,31]. However, by extending these plots to the whole range of hydrogen composition ($0 \leq r_H \leq 1.0$), one can see the fast increase in LBV at hydrogen fractions higher than 0.5. At all fractions of added H_2, the datasets obtained using the heat flux method consist of lower LBV than the present data, which were not stretch-corrected, but their trend is the same. The H_2-blended NG–air mixtures can be characterized by similar plots (Figure 2b); their LBV follows the same marked increase with r_H at hydrogen fractions higher than 0.3.

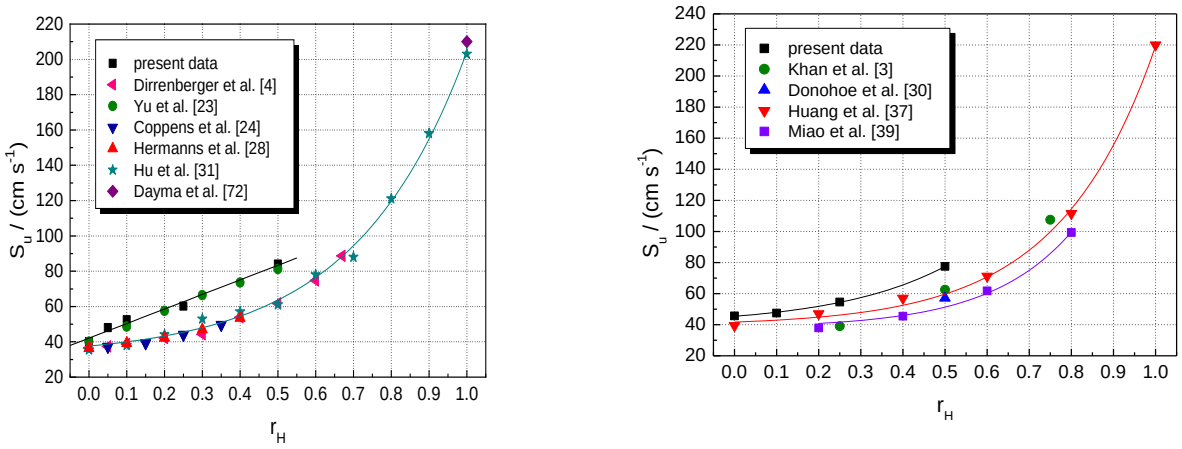

(**a**) (**b**)

Figure 2. Laminar burning velocities of single fuel–air and multifuel–air mixtures with various r_H at ambient initial pressure and temperature: (**a**) CH_4–H_2–air; (**b**) NG–H_2–air mixtures (present experimental data, in comparison with literature values).

A comparison of LBV for the stoichiometric CH_4–H_2–air and NG–H_2–air mixtures, using the present data, is shown in Figure 3 (experimental LBV) and Figure 4 (computed LBV) where the dimensionless (relative) LBV_{rel}, defined as:

$$LBV_{rel} = \frac{[S_u]_{fuel+H_2}}{[S_u]_{fuel}} \quad (5)$$

is plotted against the mole fraction of hydrogen, r_H.

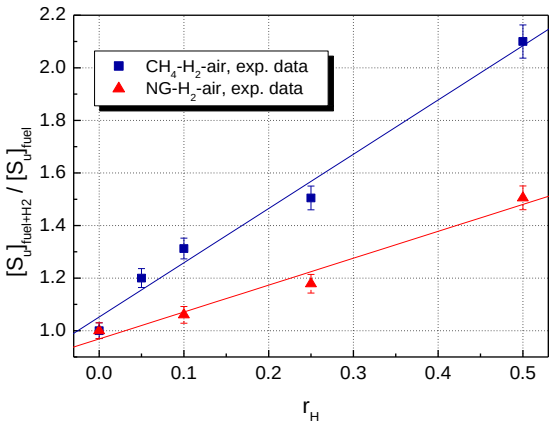

Figure 3. Experimental LBV of H_2-blended CH_4–air and NG–air with various hydrogen contents at ambient initial conditions.

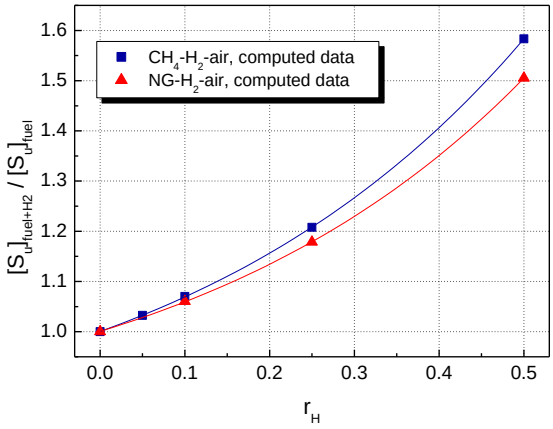

Figure 4. Computed LBV of H_2-blended CH_4–air and NG–air with various hydrogen contents at ambient initial conditions.

For both experimental and calculated datasets, H_2 addition influences to a greater extent the LBV of CH_4–air, as compared to NG–air.

For the restricted range of hydrogen fractions $0 \leq r_H \leq 0.5$, the experimental relative burning velocities $LBV_{rel} = \frac{[S_u]_{fuel+H_2}}{[S_u]_{fuel}}$ are linearly correlated with r_H. This aspect was already observed for CH_4–H_2–air and NG–H_2–air mixtures [23,36,68,69] and for other hydrogen-blended fuels as well [3,7,8,19,21,23,69,70].

At any hydrogen concentration, the burning velocities of NG–H_2–air are smaller than those of CH_4–H_2–air, as a consequence of the presence of heavier hydrocarbons in NG. Both experimental and modeling studies on the effect of hydrogen addition to the C_2, C_3, or C_4 alkanes [3,8,19–21,69,70] showed that the enhancement of LBV upon the addition of 50% H_2 was about 20–40% lower compared to when the fuel was pure methane.

The computed LBV can be compared to present experimental LBVs when plotted as functions of the equivalence ratios of H_2-blended CH_4–air and NG–air mixtures, as shown in Figure 5. The shape of the experimental (Figure 1) and computed LBVs plots is similar. The plots obtained for CH_4–H_2–air have marked maxima appearing around $\varphi = 1.10$ for all r_H. In contrast to them, the plots obtained for NG–H_2–air are rather flat; their maxima appear in the range $\varphi = 1.0$–1.10.

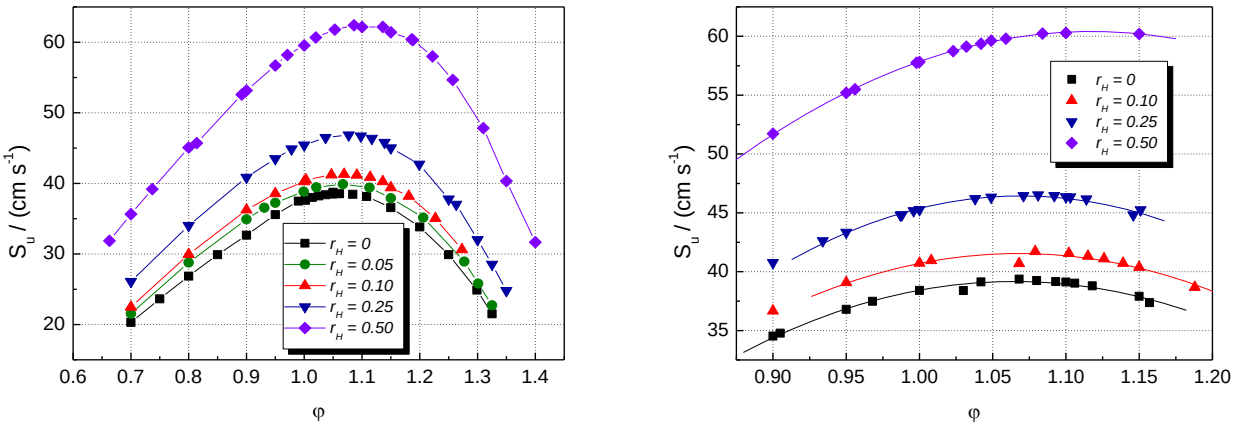

Figure 5. Computed laminar burning velocities of single fuel–air and multifuel–air mixtures with various r_H at ambient p_0 and T_0: (**a**) CH_4–H_2–air (**b**) NG–H_2–air mixtures.

Another comparison between the experimental and the computed burning velocities is shown in Figure 6 for the stoichiometric CH_4–H_2–air and NG–H_2–air mixtures with various hydrogen contents.

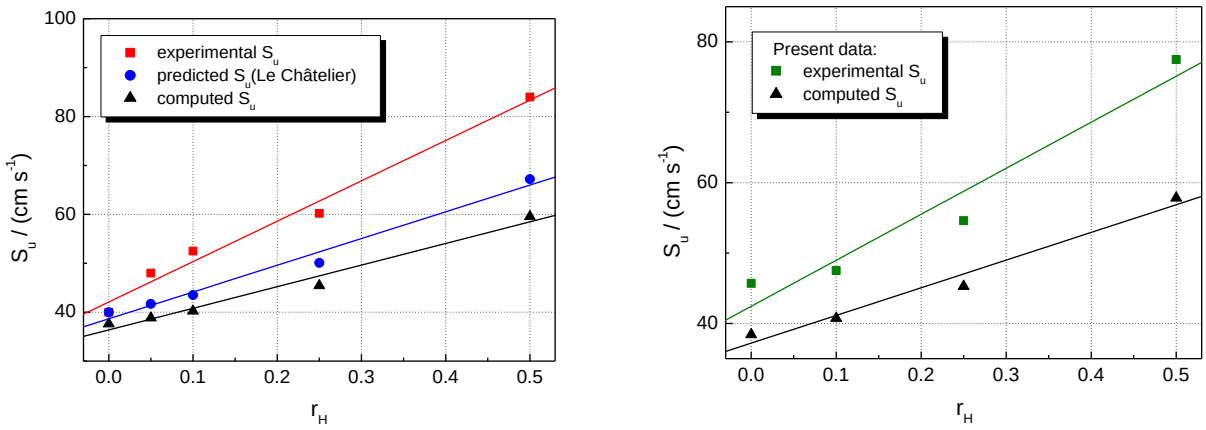

(**a**) (**b**)

Figure 6. Laminar burning velocities of stoichiometric multifuel–air mixtures with various r_H at ambient initial pressure and temperature: (**a**) CH_4–H_2–air; (**b**) NG–H_2–air mixtures.

For both CH_4 and NG mixtures, the computed LBV are lower than the experimental LBVs, and the differences increase in parallel with r_H. Figure 6a contains an additional plot of predicted LBVs, calculated from the experimental LBVs of pure H_2–air and CH_4–air mixtures and the composition of blended mixtures by using an equation proposed by Di Sarli et al. [25]:

$$S_{u,(CH_4+H_2)} = \frac{1}{\frac{r_H}{S_{u,H_2}} + \frac{1-r_H}{S_{u,CH_4}}} \quad (6)$$

The relationship is similar to Le Châtelier's rule for predicting the flammability limits of multifuel gases, using the flammability limit of each fuel from the mixture [71]. For the examined range of hydrogen concentrations, the predicted LBVs are lower than those directly obtained from experiments. However, one must consider that S_{u,H_2} used to determine the predicted LBVs were taken from the literature [71] and do not belong to the present set of experimental burning velocities.

The deviations between experimental and computed LBV can be assigned to the fact that GRI 3.0 Mech is adequate for modeling the combustion of C1–C4 alkanes (components of natural gas) but less adequate for modeling the combustion of multifuel–air mixtures with a high H_2 content. Better predictions were obtained after using improved mechanisms [19,25,28,30].

The enhancement effect of hydrogen upon flame propagation in H_2-blended mixtures can be better understood by examining the flame structure obtained from the kinetic modeling of CH_4–air and CH_4–H_2–air flames. In this purpose, the stoichiometric composition of these flammable mixtures was chosen for systems at ambient initial pressure and temperature.

The influence of H_2 concentration on temperature and the volumetric rate of heat release profiles of CH_4–H_2–air flames is shown in Figures 7 and 8 at $0 \leq r_H \leq 0.5$. The temperature of burned gas is not influenced by hydrogen addition; only the flame front thickness (evaluated as the half of the reaction zone) is decreased by H_2 addition. This variation was assigned by Salzano et al. [69] to the increased amount of NO_x produced by the combustion of H_2-blended CH_4–air ternary mixtures. In contrast to this trend, H_2 addition to CH_4–air results in a marked change in the heat release, as shown by data from Figure 8. Similar plots were obtained for H_2-blended NG–air ternary mixtures.

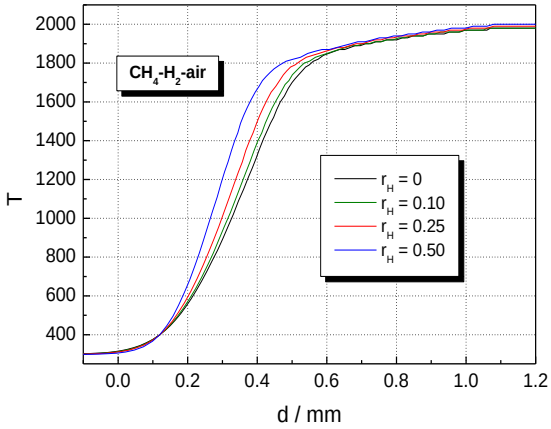

Figure 7. Computed temperature profiles in the flame front of stoichiometric CH_4–H_2–air flames with variable r_H; ambient p_0 and T_0.

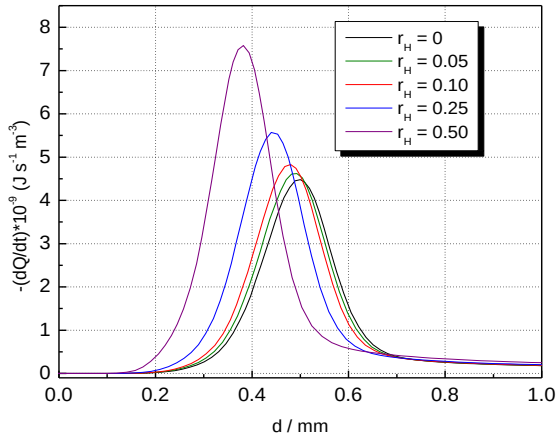

Figure 8. Volumetric rates of heat release in the flame front of CH_4–H_2–air flames with variable r_H; ambient p_0 and T_0.

The change in the volumetric rates of heat release with the fraction of added hydrogen is shown in Figure 9 for both CH_4–H_2–air and NG–H_2–air flames. Similar plots are obtained by examining r_H's influence on the sum of peak mass fractions of the most abundant radical species: H, OH, O, and HO_2, shown in Figure 10. The differences between CH_4–H_2–air and NG–H_2–air flames are observed only for mixtures with a hydrogen content below 0.25.

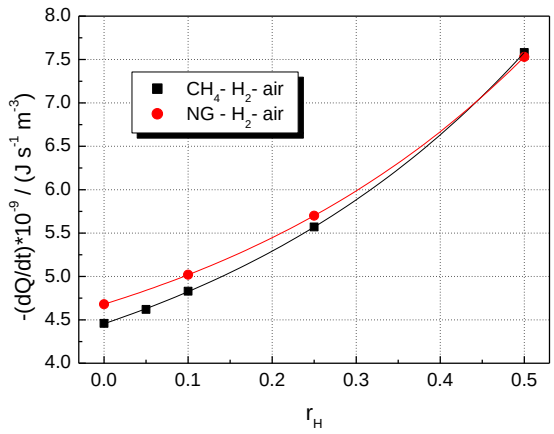

Figure 9. Influence of hydrogen fraction, r_H, on peak values of volumetric rates of heat release in the flame front of H_2-blended fuels; flames of stoichiometric mixtures at ambient p_0 and T_0.

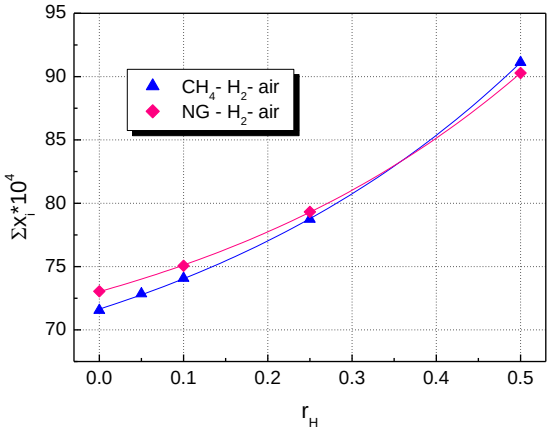

Figure 10. Influence of hydrogen fraction, r_H, on the sum of peak mass fractions from radical species, H_2-blended fuels; flames of stoichiometric mixtures at ambient p_0 and T_0.

The modeling, thus, indicates a combined (synergetic) influence of these two factors: the rate of heat release and the abundance of reactive radical species. Their individual influence on LBVs is shown in Figures 11 and 12.

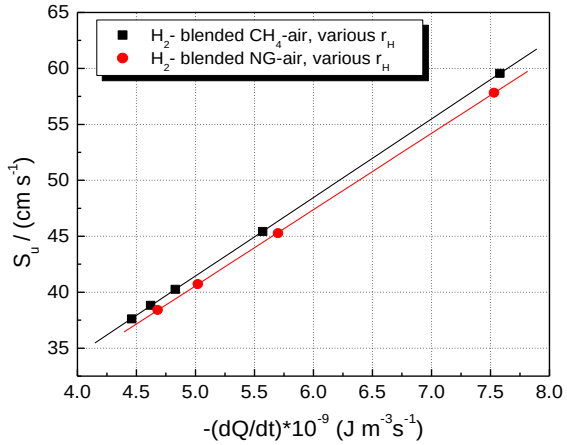

Figure 11. Experimental LBV of stoichiometric CH_4–H_2–air and NG–H_2–air mixtures in correlation with the peak values of volumetric rates of heat release; flames at ambient p_0 and T_0.

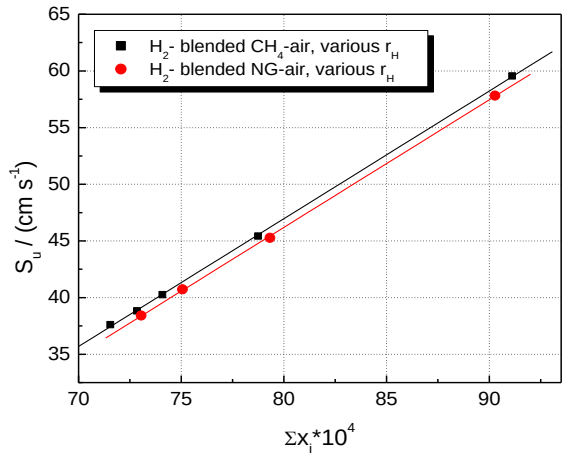

Figure 12. Experimental LBV of stoichiometric CH_4–H_2–air and NG–H_2–air mixtures in correlation with the sum of peak mass fractions of radical species; flames at ambient p_0 and T_0.

The literature data show that H_2 blending of CH_4–air or NG–air results in the enhancement of their reactivity [3,7,8,19,21,23,36–38,69,70,72,73], determining the LBV increase even if the temperature of their burned gases is little influenced by H_2 addition. The results of the present study, thus, show good agreement with previous studies on these flammable mixtures.

A less examined factor contributing to the observed variations of LBV is the thermal diffusivity of blended mixtures, which increases many folds by hydrogen addition. In accordance with the thermal theory of flame propagation, the laminar burning velocity can be written as:

$$S_u \sim \left[D \cdot C_0^{1-n} \cdot \exp\left(-\frac{E_a}{RT_f}\right)\right]^{\frac{1}{2}} \quad (7)$$

where $D = \frac{\lambda}{\rho \cdot c_p}$ is the thermal diffusivity of the flammable mixture, C_0 is the total initial fuel concentration, T_f is the end temperature in the flame front, and n and E_a are the overall activation parameters (reaction order and activation energy) of the oxidation reaction [74]. The thermophysical properties of CH_4, H_2, O_2, and N_2 are listed in Table 4. Close values are expected for NG, when compared to pure CH_4. Indeed, the high thermal conductivity of hydrogen influences the thermal diffusivity of H_2-blended CH_4–air and NG–air mixtures, resulting in higher LBVs compared to non-blended flammable mixtures.

Table 4. Heat capacities, c_p, densities, ρ, thermal conductivities, λ, and thermal diffusivities, D, of gaseous components [75].

Additive	CH_4	H_2	O_2	N_2
c_p/(J·mol^{-1}·K^{-1})	35.70	28.84	29.38	29.12
c_p/(J·kg^{-1}·K^{-1})	2231	14,420	918	1040
ρ (kg m^{-3})	0.717	0.0899	1.429	1.251
λ/(mW·m^{-1}·K^{-1})	33.0	180.5	26.6	25.8
D·10^6 (m^2 s^{-1})	20.63	129.2	20.28	19.83

6. Conclusions

The flammability characteristics of methane or natural gas enriched with hydrogen are frequently studied to ensure the safe use of these mixtures in various activity branches. Although, in practical applications, hydrogen concentration does not exceed 20%, the present study was focused on hydrogen percentages between 0 and 50% in the blended CH_4–H_2 or natural gas–H_2 mixtures.

In the study, the propagation of H_2-blended methane or natural gas–air flames in a closed spherical vessel was monitored by means of $p(t)$ variation recorded in the early stage of spherical propagation. Its novelty consists of the possibility to determine LBV from single $p(t)$ records, without additional optical methods of investigation. This simple method for evaluating data does not consider the flame stretch in this incipient stage of propagation and the flame width. However, the delivered results can be used for a preliminary characterization of the propagation stage by the LBV, extrapolated to the initial moment of experiment, i.e., at (p_0; T_0). An additional reason is based on the possibility to use the present method for multifuel- or multioxidizer-flammable mixtures, where the exact calculation of thermodynamic conditions for the burned gas, under transient conditions, is difficult, even impossible.

The experimental laminar burning velocities were examined in comparison with the computed burning velocities obtained from the numerical modeling of 1D laminar flames with the GRI 3.0 mechanism.

A fair agreement between the experimental burning velocities and reference values from the literature was observed not only for CH_4–air mixtures but for H_2-blended CH_4–air mixtures as well. The same good agreement found for present LBVs of NG–air mixtures

with literature values confirmed the possibility of using the actual simple method for extracting laminar burning velocities from the measurements of transient pressure in the early stage of explosion propagation.

The addition of increasing amounts of H_2 to CH_4 or to natural gas was found to determine the increase in laminar burning velocity for all investigated compositions of the methane–air or natural gas–air mixtures. In parallel, a strong influence of added hydrogen on the rate of heat release and concentration of active radical species in the flame front was observed. The results are assigned to the higher thermal conductivity and thermal diffusivity of hydrogen, resulting in a higher reaction rate and a higher heat dissipation rate of H_2-blended mixtures.

The reported data can further help to identify the degree of danger of explosions and develop more effective measures to prevent explosions of flammable mixtures.

Author Contributions: Conceptualization, V.S., M.M., and D.R.; methodology, M.M. and V.S.; software, M.M. and D.R.; validation, M.M. and V.S.; formal analysis, D.R.; investigation, V.S.; resources, V.S.; data curation, M.M.; writing—original draft preparation, M.M. and D.R.; writing—review and editing, M.M., D.R., and V.S. All authors have read and agreed to the published version of the manuscript.

Funding: This research received no external funding.

Institutional Review Board Statement: Not applicable.

Informed Consent Statement: Not applicable.

Data Availability Statement: Not applicable.

Acknowledgments: The present study was partially financed by the Bundesanstalt fuer Materialforschung und pruefung (BAM) and by the Romanian Academy under the scientific cooperation on flammability of complex gaseous mixtures, concluded between BAM and "Ilie Murgulescu", Institute of Physical Chemistry of the Romanian Academy.

Conflicts of Interest: The authors declare no conflict of interest.

References

1. Gad, M.S.; Ismail, M.A. Effect of waste cooking oil biodiesel blending with gasoline and kerosene on diesel engine performance, emissions and combustion characteristics. *Process Saf. Environ. Prot.* **2021**, *149*, 1–10. [CrossRef]
2. Gad, M.S.; El-Shafay, A.S.; Hashish, H.M. Assessment of diesel engine performance, emissions and combustion characteristics burning biodiesel blends from jatropha seeds. *Process Saf. Environ. Prot.* **2021**, *147*, 518–526. [CrossRef]
3. Khan, A.R.; Ravi, M.R.; Ray, A. Experimental and chemical kinetic studies of the effect of H_2 enrichment on the laminar burning velocity and flame stability of various multicomponent natural gas blends. *Int. J. Hydrogen Energy* **2019**, *44*, 1192–1212. [CrossRef]
4. Dirrenberger, P.; Le Gall, H.; Bounaceur, R.; Herbinet, O.; Glaude, P.A.; Konnov, A.; Battin-Leclerc, F. Measurements of laminar flame velocity for components of natural gas. *Energy Fuels* **2011**, *25*, 3875–3884. [CrossRef]
5. Liao, S.Y.; Jiang, D.M.; Cheng, Q. Determination of laminar burning velocities for natural gas. *Fuel* **2004**, *83*, 1247–1250. [CrossRef]
6. Zhang, B.; Xiu, G.; Bai, C. Explosion characteristics of argon/nitrogen diluted natural gas—Air mixtures. *Fuel* **2014**, *124*, 125–132. [CrossRef]
7. Ren, F.; Chu, H.; Xiang, L.; Han, W.; Gu, M. Effect of hydrogen addition on the laminar premixed combustion characteristics the main components of natural gas. *J. Energy Inst.* **2019**, *92*, 1178–1190. [CrossRef]
8. Tang, C.L.; Huang, Z.H.; Law, C.K. Determination, correlation, and mechanistic interpretation of effects of hydrogen addition on laminar flame speeds of hydrocarbon—Air mixtures. *Proc. Combust. Inst.* **2011**, *33*, 921–928. [CrossRef]
9. Brower, M.; Petersen, E.L.; Metcalfe, W.; Curran, H.J.; Fueri, M.; Bourque, G.; Aluri, N.; Guethe, F. Ignition delay time and laminar flame speed calculations for natural gas/hydrogen blends at elevated pressures. *J. Eng. Gas Turbines Power* **2013**, *135*, 021504. [CrossRef]
10. Ma, Q.; Zhang, Q.; Chen, J.; Huang, Y.; Shi, Y. Effects of hydrogen on combustion characteristics of methane in air. *Int. J. Hydrogen Energy* **2014**, *39*, 11291–11298. [CrossRef]
11. Askar, E.; Schröder, V.; Schütz, S.; Seemann, A. Power-to-gas: Safety characteristics of hydrogen/natural-gas mixtures. *Chem. Eng. Trans.* **2016**, *48*, 397–402. [CrossRef]
12. Li, T.; Hampp, F.; Lindstedt, R.P. Experimental study of turbulent explosions in hydrogen enriched syngas related fuels. *Process Saf. Environ. Prot.* **2018**, *116*, 663–676. [CrossRef]
13. Molnarne, M.; Schroeder, V. Hazardous properties of hydrogen and hydrogen containing fuel gases. *Process Saf. Environ. Prot.* **2019**, *130*, 1–5. [CrossRef]

14. Wang, T.; Zhou, Y.; Luo, Z.; Wen, H.; Zhao, J.; Su, B.; Cheng, F.; Deng, J. Flammability limit behavior of methane with the addition of gaseous fuel at various relative humidities. *Process Saf. Environ. Prot.* **2020**, *140*, 178–189. [CrossRef]
15. Zhen, X.; Tian, Z.; Wang, Y.; Liu, D.; Li, X. A model to determine the effects of low proportion of hydrogen and the flame kernel radius on combustion and emission performance of direct injection spark ignition engine. *Process Saf. Environ. Prot.* **2021**, *147*, 1110–1124. [CrossRef]
16. Chen, H.; He, J.J.; Chen, Z.M.; Geng, L.M. A comparative study of combustion and emission characteristics of dual-fuel engine fueled with diesel/methanol and diesel-polyoxymethylene dimethyl ether blend/methanol. *Process Saf. Environ. Prot.* **2021**, *147*, 714–722. [CrossRef]
17. Mitu, M.; Brandes, E.; Hirsch, W. Mitigation effects on the explosion safety characteristic data of ethanol/air mixtures in closed vessel. *Process Saf. Environ. Prot.* **2018**, *117*, 190–199. [CrossRef]
18. Dagaut, P.; Nicolle, A. Experimental and detailed kinetic modeling study of hydrogen-enriched natural gas blend oxidation over extended temperature and equivalence ratio ranges. *Proc. Combust. Inst.* **2005**, *30*, 631–638. [CrossRef]
19. Nilsson, E.J.; van Sprang, A.; Larfeldt, J.; Konnov, A.A. The comparative and combined effects of hydrogen addition on the laminar burning velocities of methane and its blends with ethane and propane. *Fuel* **2017**, *189*, 369–376. [CrossRef]
20. Kuppa, K.; Goldmann, A.; Schöffler, T.; Dinkelacker, F. Laminar flame properties of C1–C3 alkanes/hydrogen blends at gas engine conditions. *Fuel* **2018**, *224*, 32–46. [CrossRef]
21. Mosisa Wako, F.; Pio, G.; Salzano, E. The Effect of Hydrogen Addition on Low-Temperature Combustion of Light Hydrocarbons and Alcohols. *Energies* **2020**, *13*, 3808. [CrossRef]
22. Milton, B.E.; Keck, J.C. Laminar burning velocities in stoichiometric hydrogen and hydrogen- hydrocarbon gas mixtures. *Combust. Flame* **1984**, *58*, 13–22. [CrossRef]
23. Yu, G.; Law, C.K.; Wu, C.K. Laminar flame speeds of hydrocarbon+ air mixtures with hydrogen addition. *Combust. Flame* **1986**, *63*, 339–347. [CrossRef]
24. Coppens, F.H.V.; De Ruyck, J.; Konnov, A.A. Effects of hydrogen enrichment on adiabatic burning velocity and NO formation in methane+ air flames. *Exp. Therm. Fluid Sci.* **2007**, *31*, 437–444. [CrossRef]
25. Di Sarli, V.; Di Benedetto, A. Laminar burning velocity of hydrogen–methane/air premixed flames. *Int. J. Hydrogen Energy* **2007**, *32*, 637–646. [CrossRef]
26. Bourque, G.; Healy, D.; Curran, H.; Zinner, C.; Kalitan, D.; de Vries, J.; Aul, C.; Petersen, E. Ignition and Flame Speed Kinetics of Two Natural Gas Blends with High Levels of Heavier Hydrocarbons. *J. Eng. Gas Turbines Power* **2008**, *132*, 1051–1066, ASME Paper GT2008-51344. [CrossRef]
27. Tahtouh, T.; Halter, F.; Samson, E.; Mounaïm-Rousselle, C. Effects of hydrogen addition and nitrogen dilution on the laminar flame characteristics of premixed methane—Air flames. *Int. J. Hydrogen Energy* **2009**, *34*, 8329–8338. [CrossRef]
28. Hermanns, R.T.E.; Konnov, A.A.; Bastiaans, R.J.M.; De Goey, L.P.H.; Lucka, K.; Koehne, H. Effects of temperature and composition on the laminar burning velocity of CH_4 + H_2 + O_2 + N_2 flames. *Fuel* **2010**, *89*, 114–121. [CrossRef]
29. Salzano, E.; Cammarota, F.; Di Benedetto, A.; Di Sarli, V. Explosion behavior of hydrogen–methane/air mixtures. *J. Loss Prev. Process Ind.* **2012**, *25*, 443–447. [CrossRef]
30. Donohoe, N.; Heufer, A.; Metcalfe, W.K.; Curran, H.J.; Davis, M.L.; Mathieu, O.; Plichta, D.; Morones, A.; Petersen, E.L.; Güthe, F. Ignition delay times, laminar flame speeds, and mechanism validation for natural gas/hydrogen blends at elevated pressures. *Combust. Flame* **2014**, *161*, 1432–1443. [CrossRef]
31. Dayma, G.; Zhang, S.; Li, Q.F.; Pan, X.B.; Liao, S.Y.; Wang, H.Q.; Yang, C.; Wei, S. Experimental investigation on the effects of hydrogen addition on thermal characteristics of methane/air premixed flames. *Fuel* **2014**, *115*, 232–240. [CrossRef]
32. Jithin, E.V.; Varghese, R.J.; Velamati, R.K. Experimental and numerical investigation on the effect of hydrogen addition and N_2/CO_2 dilution on laminar burning velocity of methane/oxygen mixtures. *Int. J. Hydrogen Energy* **2020**, *45*, 16838–16850. [CrossRef]
33. Di Sarli, V.; Di Benedetto, A.; Long, E.J.; Hargrave, G.K. Time-Resolved Particle Image Velocimetry of dynamic interactions between hydrogen-enriched methane/air premixed flames and toroidal vortex structures. *Int. J. Hydrogen Energy* **2012**, *37*, 16201–16213. [CrossRef]
34. Di Sarli, V.; Di Benedetto, A. Effects of non-equidiffusion on unsteady propagation of hydrogen-enriched methane/air premixed flames. *Int. J. Hydrogen Energy* **2013**, *38*, 7510–7518. [CrossRef]
35. El-Sherif, S.A. Control of emissions by gaseous additives in methane—Air and carbon monoxide—Air flames. *Fuel* **2000**, *79*, 567–575. [CrossRef]
36. Huang, Z.; Zhang, Y.; Zeng, K.; Liu, B.; Wang, Q.; Jiang, D. Measurements of laminar burning velocity for natural gas-hydrogen-air-mixtures. *Combust. Flame* **2006**, *146*, 302–311. [CrossRef]
37. Huang, Z.; Zhang, Y.; Wang, Q.; Wang, J.; Jiang, D.; Miao, H. Study on flame propagation characteristics of natural gas−hydrogen−air mixtures. *Energy Fuels* **2006**, *20*, 2385–2390. [CrossRef]
38. Huang, Z.; Zhang, Y.; Zeng, K.; Liu, B.; Wang, Q.; Jiang, D. Natural gas-hydrogen-air premixed mixture combustion with a constant volume bomb. *Energy Fuels* **2007**, *21*, 692–698. [CrossRef]
39. Miao, H.; Jiao, Q.; Huang, Z.; Jiang, D. Measurement of laminar burning velocities and Markstein lengths of diluted hydrogen-enriched natural gas. *Int. J. Hydrogen Energy* **2009**, *34*, 507–518. [CrossRef]

40. Zheng, S.; Zhang, X.; Xu, J.; Jin, B. Effects of initial pressure and hydrogen concentration on laminar combustion characteristics of diluted natural gas–hydrogen—Air mixture. *Int. J. Hydrogen Energy* **2012**, *37*, 12852–12859. [CrossRef]
41. De Ferrières, S.; El Bakali, A.; Gasnot, L.; Montero, M.; Pauwels, J.F. Kinetic effect of hydrogen addition on natural gas premixed flames. *Fuel* **2013**, *106*, 88–97. [CrossRef]
42. Song, Z.; Zhang, X.; Hou, X.; Li, M. Effect of initial pressure, temperature and equivalence ratios on laminar combustion characteristics of hydrogen enriched natural gas. *J. Energy Inst.* **2018**, *91*, 887–893. [CrossRef]
43. Schroeder, V.; Askar, E.; Habib, A.K.; Tashqin, T. Sicherheitstechnische Eigenschaften von Erdgas-Wasserstoff-Gemischen. *Res. Rep. VH2539* **2016**.
44. Cellek, M.S. Flameless combustion investigation of CH_4/H_2 in the laboratory-scaled furnace. *Int. J. Hydrogen Energy* **2020**, *45*, 35208–35222. [CrossRef]
45. Ceriello, G.; Sorrentino, G.; Cavaliere, A.; Sabia, P.; de Joannon, M.; Ragucci, R. The role of dilution level and canonical configuration in the modeling of MILD combustion systems with internal recirculation. *Fuel* **2020**, *264*, 116840. [CrossRef]
46. European Standard EN 15967. *Determination of Maximum Explosion Pressure and the Maximum Rate of Pressure Rise of Gases and Vapours*; 2011.
47. Lowesmith, B.J.; Hankinson, G. Large scale high pressure jet fires involving natural gas and natural gas/hydrogen mixtures. *Process Saf. Environ. Prot.* **2012**, *90*, 108–120. [CrossRef]
48. Janès, A.; Lesage, J.; Weinberger, B.; Carson, D. Experimental determination of minimum ignition current (MIC) ratio of hydrogen/methane (H_2NG) blends up to 20 vol.% of hydrogen. *Process Saf. Environ. Prot.* **2017**, *107*, 299–308. [CrossRef]
49. Amin, M.T.; Khan, F.; Amyotte, P. A bibliometric review of process safety and risk analysis. *Process Saf. Environ. Prot.* **2019**, *126*, 366–381. [CrossRef]
50. European Standard EN 1839. *Determination of Explosion Limits of Gases and Vapours*; 2017.
51. *COSILAB*, Version 3.0.3; Rotexo-Softpredict-Cosilab GmbH & Co KG: Bad Zwischenhahn, Germany, 2012.
52. Giurcan, V.; Razus, D.; Mitu, M.; Oancea, D. Numerical study of the laminar flame propagation in ethane-air mixtures. *Cent. Eur. J. Chem.* **2014**, *12*, 391–402. [CrossRef]
53. Mitu, M.; Giurcan, V.; Razus, D.; Oancea, D. Inert gas influence on the laminar burning velocity of methane-air mixtures. *J. Hazard. Mater.* **2017**, *321*, 440–448. [CrossRef]
54. Razus, D.; Oancea, D.; Movileanu, C. Burning velocity evaluation from pressure evolution during the early stage of closed-vessel explosions. *J. Loss Prev. Process Ind.* **2006**, *19*, 334–342. [CrossRef]
55. Dobashi, R. Experimental study on gas explosion behavior in enclosure. *J. Loss Prev. Process Ind.* **1997**, *10*, 83–89. [CrossRef]
56. Knapton, J.; Stobie, I.; Krier, H. Burning Rate Studies of Fuel Air Mixtures at High Pressures. *Combust. Flame* **1973**, *21*, 211–220. [CrossRef]
57. Sapko, M.; Furno, A.; Kuchta, J. *Flame and Pressure Development of Large-Scale CH_4-Air-N_2 Explosions*; U.S. Bureau of Mines Report No. 8176; Bureau of Mines, US Department of the Interior: Washington, DC, USA, 1976.
58. Mitu, M.; Razus, D.; Giurcan, V.; Oancea, D. Normal burning velocity and propagation speed of ethane—Air: Pressure and temperature dependence. *Fuel* **2015**, *147*, 27–34. [CrossRef]
59. Razus, D.; Oancea, D.; Brinzea, V.; Mitu, M.; Movileanu, C. Experimental and computed burning velocities of propane—Air mixtures. *Energy Convers. Manag.* **2010**, *51*, 2979–2984. [CrossRef]
60. Giurcan, V.; Mitu, M.; Razus, D.; Oancea, D. Experimental study and kinetic modeling of laminar flame propagation in premixed stoichiometric n-butane-air mixture. *Rev. Chim. (Bucharest)* **2019**, *70*, 1125–1131. Available online: https://revistadechimie.ro/pdf/5%20GIURCAN%204%2019.pdf (accessed on 8 November 2021). [CrossRef]
61. Razus, D.; Mitu, M.; Giurcan, V.; Movileanu, C.; Oancea, D. Methane-unconventional oxidant flames. Laminar burning velocities of nitrogen-diluted methane–N_2O mixtures. *Process Saf. Environ. Prot.* **2018**, *114*, 240–250. [CrossRef]
62. Dahoe, A.E.; de Goey, L.P.H. On the determination of the laminar burning velocity from closed vessel gas explosions. *J. Loss Prev. Process Ind.* **2003**, *16*, 457–478. [CrossRef]
63. Metghalchi, M.A.K.J.; Keck, J.C. Laminar burning velocity of propane-air mixtures at high temperature and pressure. *Combust. Flame* **1980**, *38*, 143–154. [CrossRef]
64. Elia, M.; Ulinski, M.; Metghalchi, M. Laminar burning velocity of methane—Air–diluent mixtures. *J. Eng. Gas Turbines Power* **2001**, *123*, 190–196. [CrossRef]
65. Rahim, F.; Elia, M.; Ulinski, M.; Metghalchi, M. Burning velocity measurements of methane-oxygen-argon mixtures and an application to extend methane-air burning velocity measurements. *Int. J. Engine Res.* **2002**, *3*, 81–92. [CrossRef]
66. Razus, D.; Brinzea, V.; Mitu, M.; Movileanu, C.; Oancea, D. Burning velocity of Propane-Air Mixtures from Pressure-time Records during Explosions in a Closed Spherical Vessel. *Energy Fuels* **2012**, *26*, 901–909. [CrossRef]
67. Mitu, M.; Razus, D.; Giurcan, V.; Oancea, D. Experimental and Numerical Study of Laminar Burning Velocity of Ethane-Air Mixtures of Variable Initial Composition, Temperature and Pressure. *Energy Fuels* **2014**, *28*, 2179–2188. [CrossRef]
68. Zhang, Y.; Fu, J.; Shu, J.; Xie, M.; Liu, J. A chemical kinetic investigation of laminar premixed burning characteristics for methane-hydrogen-air mixtures at elevated pressures. *J. Taiwan Inst. Chem. Eng.* **2020**, *111*, 141–154. [CrossRef]
69. Salzano, E.; Pio, G.; Ricca, A.; Palma, V. The effect of a hydrogen addition to the premixed flame structure of light alkanes. *Fuel* **2018**, *234*, 1064–1070. [CrossRef]

70. Tang, C.; Zhang, Y.; Huang, Z. Progress in combustion investigations of hydrogen enriched hydrocarbons. *Renew. Sustain. Energy Rev.* **2010**, *30*, 195–216. [CrossRef]
71. Zabetakis, M. *Flammability Characteristics of Combustible Gases and Vapors*; No. 627; US Bureau of Mines Bull, US Department of the Interior: Washington, DC, USA, 1965.
72. Dayma, G.; Halter, F.; Dagaut, P. New insights into the peculiar behavior of laminar burning velocities of hydrogen—Air flames according to pressure and equivalence ratio. *Combust. Flame* **2014**, *161*, 2235–2241. [CrossRef]
73. Su, B.; Luo, Z.; Wang, T.; Xie, C.; Cheng, F. Chemical kinetic behaviors at the chain initiation stage of CH_4/H_2/air mixture. *J. Hazard. Mater.* **2021**, *403*, 123680. [CrossRef] [PubMed]
74. Glassman, I.; Yetter, R. *Combustion*, 4th ed.; Chapter 4; Academic Press: Burlington, MA, USA, 2008. [CrossRef]
75. Lide, D.R. CRC Handbook of Chemistry and Physics. Internet Version. 2005. Available online: http://www.hbcpnetbase.com (accessed on 9 October 2020).